Novel dye-doped cholesteric liquid crystal cone lasers with various birefringences and associated tunabilities of lasing feature and performance

Shih-Hung Lin and Chia-Rong Lee*

Institute of Electro-Optical Science and Engineering and Advanced Optoelectronic Technology Center, National Cheng Kung University, Tainan 701, Taiwan
**crlee@mail.ncku.edu.tw*

Abstract: This study is the first to investigate novel cone lasers and the tunabilities of their lasing feature and performance based on dye-doped cholesteric liquid crystal (DDCLC) films with various LC birefringences (Δn). A unique conically-symmetric lasing ring with a low energy threshold occurs at a specific nonzero oblique angle (θ_{ring}). The low energy threshold is comparable to those for common lasing signals occurring simultaneously at the short- and long-wavelength edges (SWE and LWE) of the CLC reflection band (CLCRB) for 0°. The lasing ring is induced by the enhancement in the density of photonic state for the fluorescence with a wavelength of λ_{ring} based on an edge-overlapping effect, in which λ_{ring} is just located at an edge-overlapping spectral position of the SWE of the CLCRB for 0° and the LWE of the CLCRB for θ_{ring}. The lasing feature (i.e., the lasing wavelengths of the three lasing signals and the emitted angle of the lasing ring) are tuned by varying Δn. The simulated relationship of an oblique angle with Δn, in which the SWE of the CLCRB for that oblique angle just overlaps the LWE of the CLCRB for 0°, can be obtained by calculating the dispersion relation of a planar CLC structure with various values of Δn based on Berreman's 4 × 4 matrix approach. The result of the calculation is highly consistent with the experimental data for the dependence of θ_{ring} on Δn. Furthermore, the dependence of lasing performance (energy threshold and relative slope efficiency) on Δn for the three lasing signals is also measured, which findings can be used to qualitatively identify positive interaction or competition among the three lasing signals.

OCIS codes: (230.3720) Liquid-crystal devices; (160.3710) Liquid crystals; (140.3600) Lasers,tunable; (140.3490) Lasers, distributed-feedback.

References and links

1. V. I. Kopp, B. Fan, H. K. M. Vithana, and A. Z. Genack, "Low-threshold lasing at the edge of a photonic stop band in cholesteric liquid crystals," Opt. Lett. **23**(21), 1707–1709 (1998).
2. V. I. Kopp, Z.-Q. Zhang, and A. Z. Genack, "Lasing in chiral photonic structures," Prog. Quantum Electron. **27**(6), 369–416 (2003).
3. A. Chanishvili, G. Chilaya, G. Petriashvili, R. Barberi, R. Bartolino, G. Cipparrone, A. Mazzulla, and L. Oriol, "Phototunable lasing in dye-doped cholesteric liquid crystals," Appl. Phys. Lett. **83**(26), 5353–5355 (2003).
4. A. Y.-G. Fuh, T.-H. Lin, J.-H. Liu, and F.-C. Wu, "Lasing in chiral photonic liquid crystals and associated frequency tuning," Opt. Express **12**(9), 1857–1863 (2004).
5. A. Chanishvili, G. Chilaya, G. Petriashvili, R. Barberi, R. Bartolino, G. Cipparrone, A. Mazzulla, R. Gimenez, L. Oriol, and M. Pinol, "Widely tunable ultraviolet-visible liquid crystal laser," Appl. Phys. Lett. **86**(5), 051107 (2005).
6. Y. Huang, Y. Zhou, and S.-T. Wu, "Spatially tunable laser emission in dye-doped photonic liquid crystals," Appl. Phys. Lett. **88**(1), 011107 (2006).
7. Y. Matsuhisa, Y. Huang, Y. Zhou, S.-T. Wu, Y. Takao, A. Fujii, and M. Ozaki, "Cholesteric liquid crystal laser in a dielectric mirror cavity upon band-edge excitation," Opt. Express **15**(2), 616–622 (2007).
8. K. Sonoyama, Y. Takanishi, K. Ishikawa, and H. Takezoe, "Position-sensitive cholesteric liquid crystal dye laser covering a full visible range," Jpn. J. Appl. Phys. **46**(36), L874–L876 (2007).

#149963 - $15.00 USD Received 1 Jul 2011; revised 10 Aug 2011; accepted 22 Aug 2011; published 1 Sep 2011

9. C.-T. Wang and T.-H. Lin, "Multi-wavelength laser emission in dye-doped photonic liquid crystals," Opt. Express **16**(22), 18334–18339 (2008).
10. M.-Y. Jeong, H. Choi, and J. W. Wu, "Spatial tuning of laser emission in a dye-doped cholesteric liquid crystal wedge cell," Appl. Phys. Lett. **92**(5), 051108 (2008).
11. C.-R. Lee, S.-H. Lin, H.-C. Yeh, T.-D. Ji, K.-L. Lin, T.-S. Mo, C.-T. Kuo, K.-Y. Lo, S.-H. Chang, A. Y. Fuh, and S.-Y. Huang, "Color cone lasing emission in a dye-doped cholesteric liquid crystal with a single pitch," Opt. Express **17**(15), 12910–12921 (2009).
12. C.-R. Lee, S.-H. Lin, H.-C. Yeh, and T.-D. Ji, "Band-tunable color cone lasing emission based on dye-doped cholesteric liquid crystals with various pitches and a pitch gradient," Opt. Express **17**(25), 22616–22623 (2009).
13. C.-R. Lee, S.-H. Lin, H.-S. Ku, J.-H. Liu, P.-C. Yang, C.-Y. Huang, H.-C. Yeh, and T.-D. Ji, "Optically band-tunable color cone lasing emission in a dye-doped cholesteric liquid crystal with a photoisomerizable chiral dopant," Appl. Phys. Lett. **96**(11), 111105 (2010).
14. C.-R. Lee, S.-H. Lin, H.-S. Ku, J.-H. Liu, P.-C. Yang, C.-Y. Huang, H.-C. Yeh, T.-D. Ji, and C.-H. Lin, "Spatially band-tunable color-cone lasing emission in a dye-doped cholesteric liquid crystal with a photoisomerizable chiral dopant," Opt. Lett. **35**(9), 1398–1400 (2010).
15. S.-H. Lin, C.-Y. Shyu, J.-H. Liu, P.-C. Yang, T.-S. Mo, S.-Y. Huang, and C.-R. Lee, "Photoerasable and photorewritable spatially-tunable laser based on a dye-doped cholesteric liquid crystal with a photoisomerizable chiral dopant," Opt. Express **18**(9), 9496–9503 (2010).
16. M. Humar and I. Musevic, "3D microlasers from self-assembled cholesteric liquid-crystal microdroplets," Opt. Express **18**(26), 26995–27003 (2010).
17. A. Sugita, H. Takezoe, Y. Ouchi, A. Fukuda, E. Kuze, and N. Goto, "Numerical calculation of optical eigenmodes in cholesteric liquid crystals by 4×4 matrix method," Jpn. J. Appl. Phys. **21**(Part 1, No. 11), 1543–1546 (1982).

1. Introduction

Planar cholesteric liquid crystals (CLCs) possess a one-dimensional (1D) photonic bandgap structure because of the periodic distribution of its refractive index in 1D space, wherein the rod-like LC molecules can self-organize by interacting with the chiral dopants to rotate continuously along the helical axis. If the planar CLC is doped by a fluorescence dye and is optically excited, the spontaneously emitted fluorescence from the dyes are suppressed within the stop band and enhanced at the band edges. Fluorescence photons with wavelengths at the long- and short-wavelength edges (LWE and SWE) of the CLC reflection band (CLCRB) can propagate via multi-reflection, yielding a very small group velocity and a very large density of photonic states (DOS) for the fluorescence. On the basis of the distributed feedback (DFB) effect of the fluorescence photons in the multi-reflection process of the active multilayer in the dye-doped CLC (DDCLC) cell, the rates of spontaneous and stimulated emissions at the band edges can both be amplified, so that a high gain can exceed the loss to induce low-threshold lasing emission [1,2].

In the past decade, DDCLC lasers have been widely investigated because of the significance of their edge lasing mechanism [1,2] and their potential applications [3–16]. Particularly, in our recent work we observed a novel lasing phenomenon, a color cone lasing emission (CCLE), based on a single-pitched DDCLC cell [11]. The lasing wavelength in the CCLE is distributed continuously within a wide-band, as measured at a continuously increasing cone angle relative to the helical axis along the cell normal. Further applications of band-tunable color cone lasers, in which the CLC pitch is varied and the LC birefringence (Δn) is fixed, were also developed [12–14]. The current work is the first to report a novel DDCLC cone lasers with various Δn and associated lasing feature and performance tunabilities. Experimental results reveal that a novel conically-symmetric lasing ring (seen on the screen) with a low energy threshold can be obtained at a specific nonzero oblique angle (θ_{ring}) based on a DDCLC cell. The threshold is comparable to those for common normal lasing signals emitted simultaneously at the SWE and LWE for 0°. Such a lasing ring is attributable to the DOS enhancement of the fluorescence with a wavelength of λ_{ring} based on an edge-overlapping effect, in which λ_{ring} coincides with the edge-overlapping spectral position of the LWE of the CLCRB measured at θ_{ring} and the SWE of the CLCRB measured at 0°. The wavelengths of the lasing ring and lasing signals at the SWE and LWE for 0° and the emitted oblique angle of the lasing ring are tuned by changing the Δn of LCs. The simulated relationship of an oblique angle ($\theta_{overlap}$) with Δn, in which the SWE of the CLCRB for that oblique angle just overlaps the LWE of the CLCRB for 0°, can be obtained by calculating the

#149963 - $15.00 USD Received 1 Jul 2011; revised 10 Aug 2011; accepted 22 Aug 2011; published 1 Sep 2011

dispersion relation for planar CLC structures using Berreman's 4 × 4 matrix method. The simulation result agrees well with the experimental result for the dependence of θ_{ring} on Δn. In addition, the relationship between the lasing performance (i. e., energy threshold and relative slope efficiency) and Δn for the three lasing signals are also obtained, which findings can used accordingly to qualitatively identify positive interaction or competition among the three lasing signals.

2. Sample preparation and experimental setups

The DDCLC materials used include four different nematic LCs (NLCs), LCT-06-99 (n_e = 1.5485 and n_o = 1.4693 at 20 °C), MDA-03-3970 (n_e = 1.6309 and n_o = 1.4987 at 20 °C), MDA-04-606 (n_e = 1.7153 and n_o = 1.5086 at 20 °C), and MDA-98-1602 (n_e = 1.7779 and n_o = 1.5113 at 20 °C) (all from Merck), a left-handed chiral dopant, S811 (from Merck), and a laser dye, Pyrromethene 597 (P597) (from Exciton). Each empty cell is pre-fabricated with the same standard by combining two indium-tin-oxide-coated glass slides separated by two 23 μm-thick plastic spacers. Both glass slides in each empty cell are pre-coated with polyvinyl alcohol film and pre-rubbed in anti-parallel direction. Eight DDCLC mixtures with different prescriptions (Table 1) are prepared and injected into eight identical empty cells to form eight different DDCLC cells marked cells 1–8. These cells are then placed together in a clean and opaque specimen box at room temperature for about one week to enable the CLC in each cell to have sufficient time to gradually self-organize into a perfect planar structure. In addition to the DDCLC prescription, other optical information on these cells is also provided in Table 1. Examples include the value of the birefringence of LCs, helical pitch, and wavelengths at the LWE and SWE of CLCRB at 0° [$\lambda_{LWE}(0°)$ and $\lambda_{SWE}(0°)$, respectively]. All the DDCLC cells are divided into two groups for cells 1–4 and 5–8 with increasing birefringence of Δn_1–Δn_4. The $\lambda_{LWE}(0°)$ for each cell in group I and the $\lambda_{SWE}(0°)$ for each cell in group II are pre-designed to be located at the wavelengths of 639.9 and 575.0 nm, respectively.

Table 1. Two groups for the eight DDCLC cells with different prescriptions and optical parameters [e. g., birefringence of LCs (Δn), pitch and wavelengths at LWE and SWE of CLCRB for 0°, $\lambda_{LWE}(0°)$, and $\lambda_{SWE}(0°)$, respectively]

Group	Cell	Prescription of DDCLC NLC: chiral dopant: laser dye (wt.%)	Birefringence of LCs, Δn	Pitch (nm)	$\lambda_{LWE}(0°)$ (nm)	$\lambda_{SWE}(0°)$ (nm)
I	1	LCT-06-99: S811: P597 = 77.8: 21.7: 0.5	$\Delta n_1 = 0.0792$	$P_1 = 412.6$	639.9	605.8
	2	MDA-03-3970: S811: P597 = 77.3: 22.2: 0.5	$\Delta n_2 = 0.1322$	$P_2 = 394.7$	639.9	596.6
	3	MDA-04-606: S811: P597 = 76.6: 22.9: 0.5	$\Delta n_3 = 0.2067$	$P_3 = 377.8$	639.9	580.2
	4	MDA-98-1602: S811: P597 = 74.2: 25.3: 0.5	$\Delta n_4 = 0.2666$	$P_4 = 366.1$	639.9	568.1
II	5	LCT-06-99: S811: P597 = 76.6: 22.9: 0.5	$\Delta n_1 = 0.0792$	$P_5 = 391.8$	607.8	575.0
	6	MDA-03-3970: S811: P597 = 76.4: 23.1: 0.5	$\Delta n_2 = 0.1322$	$P_6 = 380.2$	616.0	575.0
	7	MDA-04-606: S811: P597 = 76.4: 23.1: 0.5	$\Delta n_3 = 0.2067$	$P_7 = 374.3$	634.2	575.0
	8	MDA-98-1602: S811: P597 = 74.5: 25.0: 0.5	$\Delta n_4 = 0.2666$	$P_8 = 370.7$	648.3	575.0

In the experiment, two setups are utilized for measuring the lasing and transmission spectra (complementary to the reflection spectra) of the DDCLC cells. Associate setups and methods for measurement can be found in our recent published work [11]. In brief, the DDCLC cell is excited by a single incident pumped pulses beam originating from a Q-switched Nd:YAG SHG pulse laser with a wavelength of 532 nm, a pulse duration of 8 ns, a repetition rate of 10 Hz, and a pumped energy of E, at an incident angle of roughly 15° from the cell normal (**N**). The lasing signals can then be generated and measured behind the cell at a distance of ~4 cm from the pumped spot on the cell. To analyze the lasing signals emitted from one of the DDCLC cells with different Δn at a specific oblique angle from **N**, the transmission spectrum of that cell, which reveals the band structure of the corresponding CLC structure, is measured at the same angle. Both the lasing and transmission spectra of each cell are measured using the same system of the fiber-based spectrometer (Jaz-combo-2, optical resolution ~0.9 nm, Ocean Optics).

#149963 - $15.00 USD Received 1 Jul 2011; revised 10 Aug 2011; accepted 22 Aug 2011; published 1 Sep 2011

3. Results and discussion

Figure 1 shows the measured absorption and spontaneously emitted fluorescence spectra of 0.5 wt.% P597 solved in the four kinds of LCs with Δn_1–Δn_4 (represented by the red, green, blue, and violet curves, respectively). The experimental result in this figure shows that the four spectral curves of the laser dye for absorption or fluorescence emission are almost identical. The peaks for any one of the absorption and fluorescence emission spectra are located at nearly the wavelength positions of 526 and 575 nm, respectively. The absorption and fluorescence emission for the laser dye almost vanish and can be neglected if the wavelength position is higher than 578 and 700 nm, respectively.

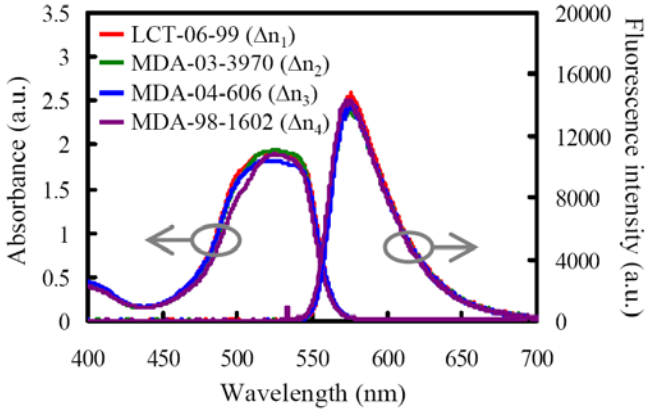

Fig. 1. Measured absorption and fluorescence emission spectra of 0.5 wt.% P567 solved in four kinds of LCs with different birefringences of Δn_1–Δn_4 (LCT-06-99, MDA-03-3970, MDA-04-606, and MDA-98-1602, respectively), indicated by the red, green, blue, and violet curves, respectively.

In our previous work, we demonstrated the existence of the CCLE based on several perfect planar DDCLC cells with different pitches and identical Δn [12]. The experimental results in that study showed that in addition to the common lasing spots exhibited at 0° (called the normal lasing signals along **N**) at the LWE and SWE of CLCRB for 0°, a novel lasing ring exhibited at around 35° from **N** at the LWE of CLCRB for 35° for the DDCLC cells can also be easily observed by the naked eye. The lasing signals emitted at other nonzero oblique angles were much weaker than those emitted at 0° and 35°, so that only a sensitive spectrometer can detect them. The lasing ring mentioned in Ref. [12] is particularly worthy of further investigation because no similar lasing phenomenon has ever been reported and investigated thus far in other DFB laser systems fabricated with materials that differ from DDCLC (e. g., metals, semiconductors, polymers and their composites, and LC-polymer mixtures). Interestingly, preliminary findings have shown that the generation of the 35° lasing ring was associated with the location of the lasing wavelength, λ_{ring}, just at the edge-overlapping wavelength position of the LWE of the CLCRB for 35° and the SWE of the CLCRB for 0° [i.e., $\lambda_{LWE}(35°) = \lambda_{SWE}(0°)$] for all the DDCLC cells with identical Δn and different pitches. The edge-overlapping effect may induce the DOS enhancement in the fluorescence emission with a wavelength of $\lambda_{LWE}(35°) = \lambda_{SWE}(0°)$, thereby dramatically improving the lasing intensity and decreasing the energy threshold for the lasing signals emitted at 35°. In addition, we infer that the enhanced fluorescence emission with $\lambda_{LWE}(35°) = \lambda_{SWE}(0°)$ propagating at 35° may also induce fluorescence enhancement with the same wavelength propagating at 0° and vice versa. More evidence based on DDCLC cells with different Δn are presented later in the paper to provide clear support for this positive interaction between the lasing ring with λ_{ring} and the lasing signal at the SWE for 0°.

To further investigate the anomalous lasing ring and its relationship with the normal lasing signals, as well as develop possible manipulations in their application, we focus on studying

#149963 - $15.00 USD Received 1 Jul 2011; revised 10 Aug 2011; accepted 22 Aug 2011; published 1 Sep 2011

the dependence of the lasing features (lasing wavelength and emitted oblique angle) on Δn based on the DDCLC cells with different Δn presented in Table 1. In addition, the variations in lasing performance (energy threshold and relative slope efficiency) are also measured and studied. Figures 2(a.1)–2(a.8) show the obtained lasing patterns on the screen after cells 1–8 are individually excited by incident pumped pulses with the same amount of energy at E = 8 μJ/pulse. Clearly, in addition to the common normal lasing spots exhibited at 0°, four bright lasing rings with different colors (the same colors) at 29°, 34.6°, 43.6°, and 50° for cells 1–4 (5–8), respectively, can also be observed. The corresponding lasing and transmission spectra for the normal lasing signals at 0° and the lasing rings at 29°, 34.6°, 43.6°, and 50° based on cells 1–4 (5–8) are measured and displayed in Figs. 2(b.1)–2(b.4) [2(b.5)–2(b.8)], respectively. The formation of all the lasing rings for all the cells are directly associated with the edge-overlapping effect. That is, the lasing rings at 29°, 34.6°, 43.6°, and 50° for cells 1–4 (5–8), respectively, occur at the edge-overlapping wavelength position of the SWE of CLCRB for 0° and the LWE of CLCRB for 29°, 34.6°, 43.6°, and 50° based on cells 1–4 (5–8), respectively. Experimental data on the variations in the edge-overlapping wavelength of the lasing ring and lasing signal at the SWE of CLCRB for 0° [i. e. $\lambda_{ring} = \lambda_{las,SWE}(0°)$] based on cells 1–4, the variation in the wavelength of the lasing signal at the LWE of CLCRB for 0° [$\lambda_{las,LWE}(0°)$] based on cells 5–8, and the variation in the emitted oblique angle of the lasing ring (θ_{ring}) for cells 1–4 or 5–8 with Δn of the LCs in Fig. 2 are summarized in Figs. 3(a) (indicated by the blue and red filled dots, respectively) and 3(b) (indicated by the filled red diamond). Experimental data in Fig. 3 presents the tunability of the lasing feature for the DDCLC laser with changes in LC birefringence. As shown in the blue curve of Figs. 3(a) and 2(b.1)–2(b.4), because the LWE of the CLCRB for 0° based on cells 1–4 is fixed at 639.9 nm, the $\lambda_{las,LWE}(0°)$ is also fixed at 639.9 nm but $\lambda_{ring} = \lambda_{las,SWE}(0°)$ increasingly blue-shifts from 605.8 to 568.1 nm (light red → green) with increasing Δn from 0.0792 to 0.2666. By contrast, because the SWE of the CLCRB for 0° based on cells 5–8 is fixed at 575.0 nm, $\lambda_{ring} = \lambda_{las,SWE}(0°)$ is also fixed at 575.0 nm but $\lambda_{las,LWE}(0°)$ increasingly red-shifts from 607.8 to 648.3 nm (light red → deep red) with increasing Δn from 0.0792 to 0.2666, as displayed in the red curve of Figs. 3(a) and 2(b.5)–2(b.8). Experimental data in Fig. 3(b) indicate that a linear increase in θ_{ring} occurs with increasing Δn. In accordance with a similar simulation step described in our previous study [11], the simulation result for dispersion relations (obtained using Berreman's 4 × 4 matrix approach) for a planar CLC structure [17] with various values of Δn yields the simulated oblique angles ($\theta_{overlap}$). In these angles, the LWE of the corresponding CLCRB overlaps with the SWE of the CLCRB for 0° [represented by the open diamond ◇ in Fig. 3(b)]. High consistency between the experimental and simulation results [i.e., $\theta_{ring}(\Delta n)$ and $\theta_{overlap}(\Delta n)$, respectively] can be obtained. This consistency confirms the validity of the edge-overlapping effect in the formation mechanism of the unique lasing rings.

Figures 2(c.1)–2(c.4) [2(c.5)–2(c.8)] show the plot of the variations in the intensity of the lasing signal at the LWE and SWE of the CLCRB for 0°, indicated by black and pink dots, respectively. Also shown are the lasing signal at the LWE of the CLCRB for θ_{ring} = 29°, 34.6°, 43.6°, and 50°, indicated by dots, red, green, blue, and purple dots, respectively, based on cells 1–4 (5–8), respectively, with incident pumped energy. Experimental results in Figs. 2(c.1)–2(c.4) [2(c.5)–2(c.8)] are summarized in Figs. 4(a) and 4(b) [5(a) and 5(b)]. These figures plot the variations in the energy threshold and relative slope efficiency (arbitrary unit, defined as the ratio of the lasing intensity to the incident pumped energy shown in Fig. 2) for the DDCLC lasers with the lasing wavelengths of $\lambda_{las,LWE}(0°)$, $\lambda_{las,SWE}(0°)$, and λ_{ring} (represented by diamond, triangular, and circular dots, respectively). The experimental data in Figs. 4 and 5 present the tunability of the lasing performance for the DDCLC laser with changing LC birefringence. According to the experimental results in these figures, several peculiar features of the three edge lasing signals and their relationships for the DDCLC lasers based on cells 1–4 or 5–8 can be qualitatively identified and explained as follows. First, the dependence of the performance of the lasing signals with λ_{ring}, $\lambda_{las,SWE}(0°)$, and $\lambda_{las,LWE}(0°)$ on the Δn for cells 1–4 or 5–8 is dominated primarily by the spectral distribution of the

#149963 - $15.00 USD Received 1 Jul 2011; revised 10 Aug 2011; accepted 22 Aug 2011; published 1 Sep 2011

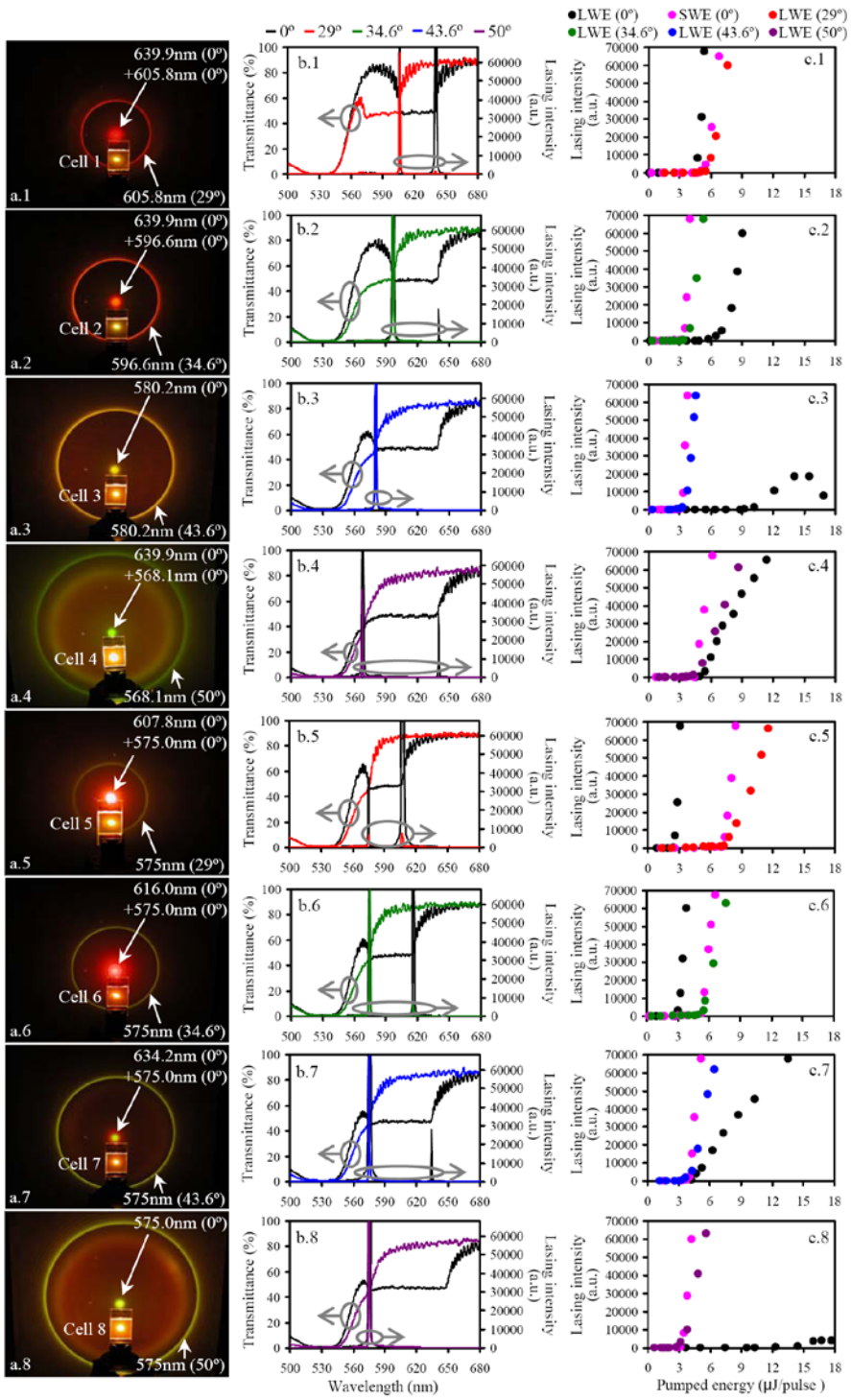

Fig. 2. (a.1)–(a.4) [(a.5)–(a.8)] Obtained lasing patterns and (b.1)–(b.4) [(b.5)–(b.8)] the measured lasing and transmission spectra at E = 8 μJ/pulse; (c.1)–(c.4) [(b.5)–(b.8)] the variations in the lasing intensity with the incident pumped energy for lasing signals at the LWE and SWE for 0° and at the LWE for 29°, 34.6°, 43.6°, and 50° based on DDCLC cells 1–4 (5–8) with Δn_1–Δn_4, respectively.

#149963 - $15.00 USD Received 1 Jul 2011; revised 10 Aug 2011; accepted 22 Aug 2011; published 1 Sep 2011

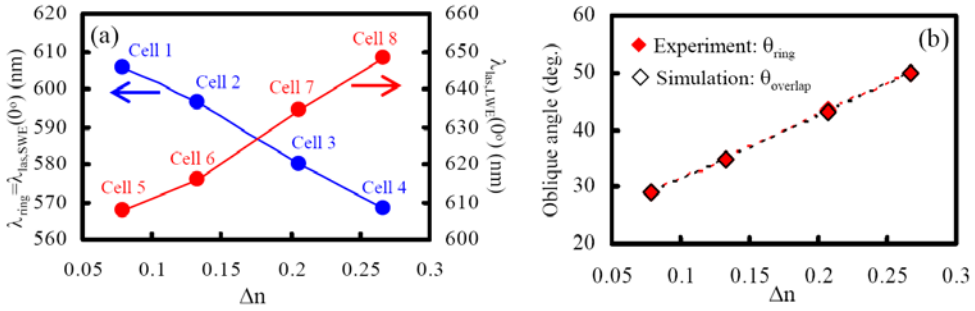

Fig. 3. (a) Variation in the edge-overlapping wavelength of the lasing ring and the lasing at the SWE for 0° [$\lambda_{ring} = \lambda_{las,SWE}(0°)$] with Δn based on cells 1–4 (represented by blue dots), and that in the wavelength of the lasing at the LWE for 0° [$\lambda_{las,LWE}(0°)$] with Δn based on cells 5–8 (represented by red dots). (b) Variation in the emitted oblique angle for the lasing ring (θ_{ring}) with Δn in the experiment (represented by red diamonds), and that in the simulated oblique angle ($\theta_{overlap}$) in which the LWE of the corresponding CLCRB overlaps with the SWE of the CLCRB for 0° with Δn in the simulation (represented by open diamonds) based on cells 1–4 or 5–8.

spontaneously emitted fluorescence intensity (attached blue curve, Fig. 4 or 5). Thus, the energy threshold and relative slope efficiency for the lasing signal with λ_{ring} or $\lambda_{las,SWE}(0°)$ [with $\lambda_{las,LWE}(0°)$] increases and decreases, respectively, when the fluorescence intensity decreases for cells 1–4 (5–8). Second, for a laser based on any one of cells 1–4 or 5–8, the energy threshold (relative slope efficiency) for the lasing ring with λ_{ring} is always higher (lower) than that for the lasing signal with $\lambda_{las,SWE}(0°)$ even though $\lambda_{las,SWE}(0°)$ equals λ_{ring}. This is reasonable because according to the previous result displayed in the last figure in Ref. [11], the emission rates of the fluorescence associated with the lasing ring are generally lower than those associated with the lasing signal for 0°. This phenomenon may be attributed to two factors: the smaller effective transition dipole moment of laser dyes in absorption and the stronger scattering of fluorescence light propagating at a nonzero oblique angle. Third, when the performance for the lasing signals with λ_{ring} and $\lambda_{las,SWE}(0°)$ coherently increase (decrease)

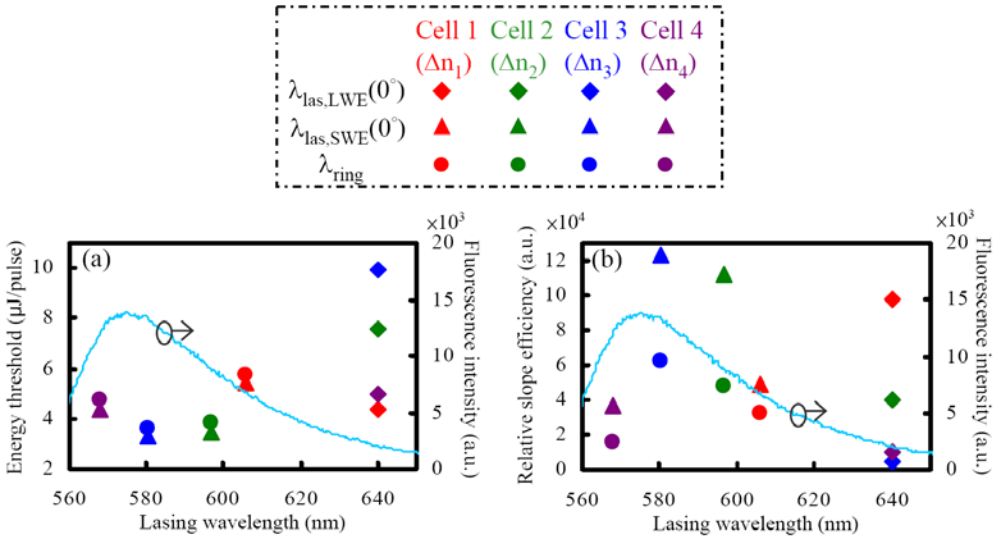

Fig. 4. Variations in (a) the energy threshold and (b) the relative slope efficiency with Δn for the lasing signals with $\lambda_{las,LWE}(0°)$, $\lambda_{las,SWE}(0°)$, and λ_{ring} (represented by diamond, triangular, and circular dots, respectively) based on cells 1–4. The blue curve in (a) and (b) represents the fluorescence emission spectrum of the laser dye.

#149963 - $15.00 USD Received 1 Jul 2011; revised 10 Aug 2011; accepted 22 Aug 2011; published 1 Sep 2011

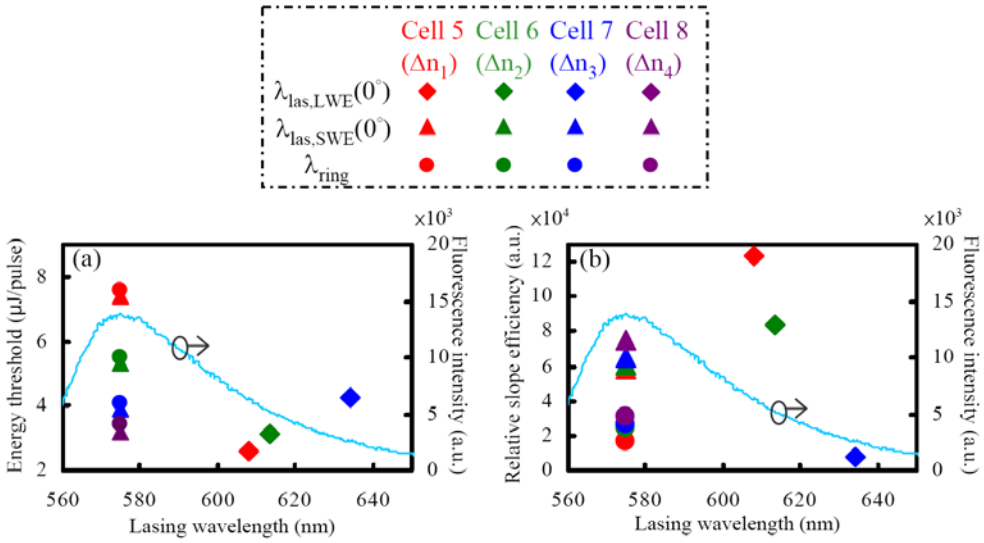

Fig. 5. Variations in (a) the energy threshold and (b) the relative slope efficiency with Δn for the lasing signals with $\lambda_{las,LWE}(0°)$, $\lambda_{las,SWE}(0°)$, and λ_{ring} (represented by diamond, triangular, and circular dots, respectively) based on cells 5–8. The blue curve in (a) and (b) represents the fluorescence emission spectrum of the laser dye.

with increasing Δn, that for the third lasing signal with $\lambda_{las,LWE}(0°)$ always decreases (increases) with increasing Δn based on cells 1–4 or 5–8. This result clearly confirms two relationships among the three lasing signals: positive interaction between the two lasing signals with λ_{ring} and $\lambda_{las,SWE}(0°)$ and their competition with the third signal with $\lambda_{las,LWE}(0°)$. These relationships result in the coherent variations in the first two lasing signals, and their variations reversed to that for the third with increasing or decreasing Δn.

4. Conclusion

In summary, this investigation is the first to report novel DDCLC cone lasers with different Δn, as well as their lasing characteristics and performance tunabilities. In addition to the common lasing signals generated simultaneously at the SWE and LWE for 0°, one particular lasing ring is generated at a specific nonzero oblique angle (θ_{ring}) because of DOS enhancement of the fluorescence with a wavelength of λ_{ring} based on an edge-overlapping effect. In this effect, λ_{ring} just coincides with an edge-overlapping spectral position of the SWE of the CLCRB for 0° and the LWE of the CLCRB for θ_{ring}. The lasing wavelength and emitted angle for the lasing ring are changeable with the variations in Δn. In the simulated relationship of an oblique angle with the Δn, in which the SWE of the CLCRB for that oblique angle superimposes the LWE of the CLCRB for 0°, can be obtained by calculating the dispersion relation for a planar CLC structure with different values of Δn based on Berreman's 4 × 4 matrix approach. The results of the calculation are in good agreement with the experimental findings on the dependence of θ_{ring} on Δn. Moreover, the dependence of the energy threshold and relative slope efficiency on Δn for the lasing signals are also measured and discussed. Work devoted to the development of a spatially tunable cone laser based on a DDCLC cell with a gradient of birefringence is currently underway.

Acknowledgments

The authors would like to thank the National Science Council of the Republic of China, Taiwan (Contract No. NSC 100-2112-M-006-012-MY3) and the Advanced Optoelectronic Technology Center, National Cheng Kung University, under projects from the Ministry of Education for the financial support. We greatly appreciate the editorial assistance extended by KGSupport.

#149963 - $15.00 USD Received 1 Jul 2011; revised 10 Aug 2011; accepted 22 Aug 2011; published 1 Sep 2011